Instrumented Fragment Impact Testing for Reactive Burn Model Validation

Author: Magnus Bergh, Swedish Defence Research Agency
Email: magnus.bergh@foi.se

ABSTRACT

Instrumented fragment impact tests have been performed in order to validate previously performed calibration of a reactive burn model parameter set for the explosive PBXN-109. In these tests, the fragment velocity was set specifically to facilitate model validation and the charge was instrumented with a PDV-probe to monitor expansion velocity of the charge casing. The reactive response was also evaluated through high-speed video recording, charge fragment analysis and blast pressure measurements. It was found that the critical fragment velocity for this PBXN-109 composition is around 1820 m/s and that the previously calibrated model over-predicts this threshold by 150 m/s. Furthermore, a recalibration is performed which reproduces the measured critical fragment velocity while preserving a fair agreement with previous experimental data.

INTRODUCTION

Minimizing the risk of advertent initiation of munitions is important for vehicle survivability during in-theatre operations. On the battlefield, a munitions response to an impacting fragment inside a vehicle can make the difference between a minor incident and kill. Fundamental understanding of the physical and chemical processes, which govern this response, is decisive in the design and assessment of insensitive munitions.
In previous work [1], reactive burn model parameters where calibrated against initiation experiments. This calibration included first gap tests instrumented with manganin gauges providing pressure histories at various positions in the explosive and secondly rate stick tests providing data on detonation velocity and detonation front curvature as function of charge diameter. It was concluded that fair agreement against both sets of tests could be obtained with a single parameter set. It is, however, challenging to obtain high accuracy against pressure histories and simultaneously capturing the diameter effect, specifically the curvature of the detonation front at small diameters approaching the critical diameter.
In the present study, fragment impact tests have been performed on a generic cylindrical cased charge containing PBXN-109, with the aimpoint at the centre of the cylinder base. In addition to conventional diagnostic equipment such as high-speed video recording and blast pressure measurements, the tests were instrumented with a Photon Doppler Velocimeter (PDV). This realizes a direct comparison to hydrocode initiation simulations, allowing us to perform efficient model validation of the previously calibrated reactive burn model parameter set.
Before the fragment impact tests were performed, a hydrocode model of projectile and charge was constructed, allowing us to estimate suitable fragment velocities and predict an approximate threshold for initiation. Based on the ALE formalism in LS-Dyna, this model includes all components of projectile and charge in 3D with the explosive described by the ignition and growth model. Such a 3D model allows us to explore effects such as projectile jaw, which has been identified as important elsewhere [1].

EXPERIMENT

Since our goal is to obtain fundamental understanding and to perform model validation, we pick a charge design with a simple geometry: a cylindrical charge with a 6 mm steel casing. The charge casings were machined with one end open. The explosive was cast in this

cylindrical container with threads at the open casing end, allowing a cap to be screwed on after machining of the explosive. A drawing of the container with cap is provided in Figure 1.

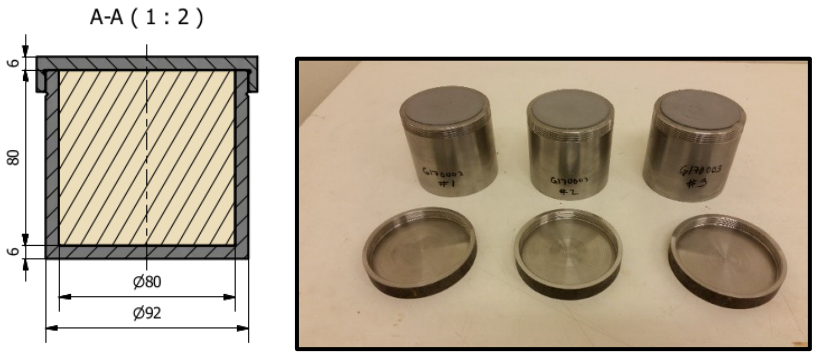

Figure 1. Drawing of the charge (left) and photograph of machined charges with caps off.

Three charges were manufactured for fragment impact testing. It was considered important to obtain a high quality cast without any cavities, in particular at the explosive-casing boundary on the impact side. The PBXN-109 explosive was cast with vibration but not under vacuum. Fragments for the test were machined according to the STANAG 4496 dimensions. It has a diameter of 14.30 mm, length of 15.56 mm (nose to back) and a 10˚ conical nose. The mass is close to 18.4 g.

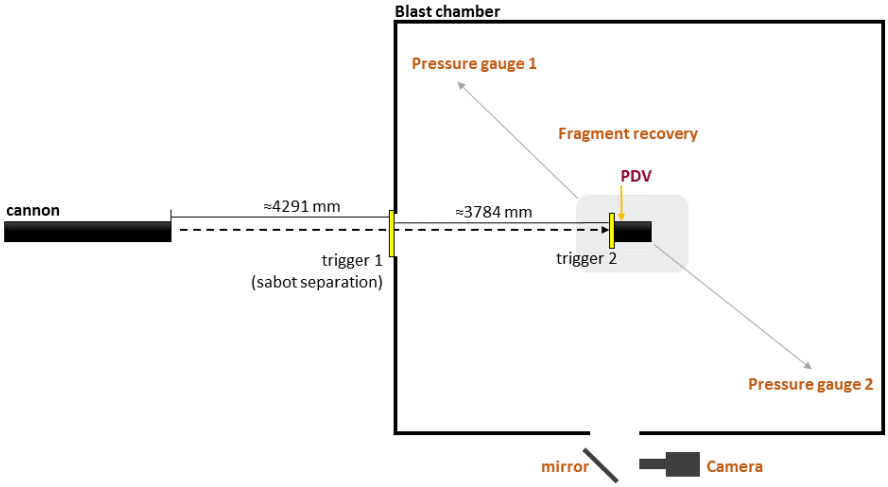

Figure 2. Drawing of experimental setup.

The fragment was fired into a blast chamber to eliminate the risk of spreading reacting explosive into the surrounding environment. Figure 2 shows a schematic drawing of the test setup. The cannon (30 mm smooth bore) fires the fragment through a hole into the blast chamber. At the blast chamber wall, the sabots are separated and the fragment triggers a foil providing a time of arrival (trigger 1). A second trigger foil is positioned on the charge (trigger 2) and thus an approximate fragment velocity can be calculated. The second foil also acts as a trigger for the PDV. The impact of the fragment on the charge is recorded using a high-speed camera situated outside the blast chamber. To protect the camera, a mirror is used to reflect light from the impact region into the camera behind the blast chamber wall. Two pressure gauges were positioned in two opposing corners of the chamber. A stack of cardboard was used to recover charge fragments after a violent response.

MODEL DESCRIPTION

In order to be able to capture effects such as a tilted fragment, a 3D ALE model has been constructed in LS-Dyna. We use Lagrange formulation for the fragment, Euler formulation for

the charge and fluid-structure-interaction with penalty-based contacts to handle the interaction between these parts. Transformation commands are utilized to rotate and translate the fragment arbitrarily in **x** and **y** (fragment velocity vector along **z**). For tilt in one plane only and impact at the centre point, we use a half-model with a symmetry plane. The timestep is reduced just after impact to minimize leakage of material through the boundaries.

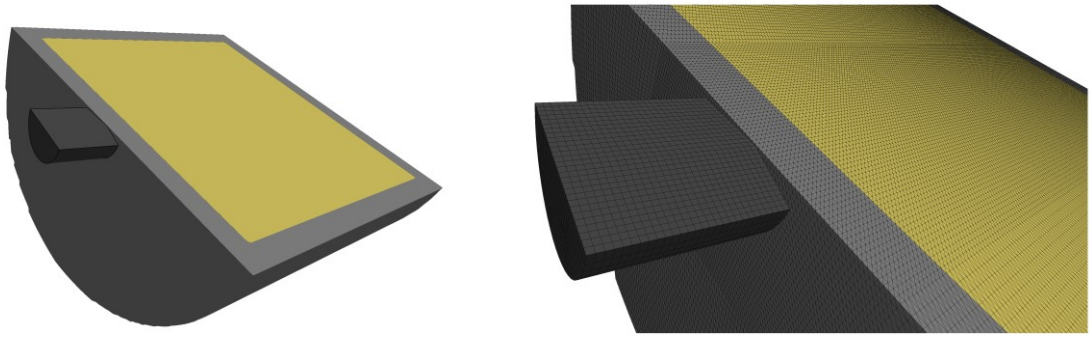

Figure 3. 3D ALE model of fragment (dark gray), casing (light gray) and explosive (yellow). The right part of the figure shows the computational mesh.

Figure 3 shows the ALE model with a 5˚ yaw (left). The right part of the figure shows the computational mesh. Tracer particles are attached to the nodes at the positions corresponding to PDV and pins. As the casing expands, tracer particle position is recorded every 10:th nanosecond. The casing may be displaced in the axial direction **z** during expansion. Movement of the tracer particles in the axial direction results in an offset between simulated expansion velocity and the PDV signal. This effect is however very small since the detonation front impacts the inside of the casing almost at normal incidence.
A 2D model is utilized to check mesh convergence with respect to critical fragment velocity. The critical velocity is preserved to within 2% when the element size is increased from 0.2 mm to 0.5 mm. An element size of 0.5 mm is used in the 3D model.
For the explosive, we used the Ignition and growth equation of state model with the parameters obtained in the previous study [2]. In this calibration, the burn parameters where calibrated against both instrumented gap tests and rate stick tests. For the steel fragment and casing we use Johnson-cook plasticity model with parameters from Wang [3].

MODEL DEMONSTRATION

First, we demonstrate how the model can be used to simulate various effects in the current fragment impact setup. We consider a fragment with a velocity of 1700 m/s and a 5˚ tilt in the horizontal plane. Since the tilt is in one direction only, a half 3D-model is sufficient.

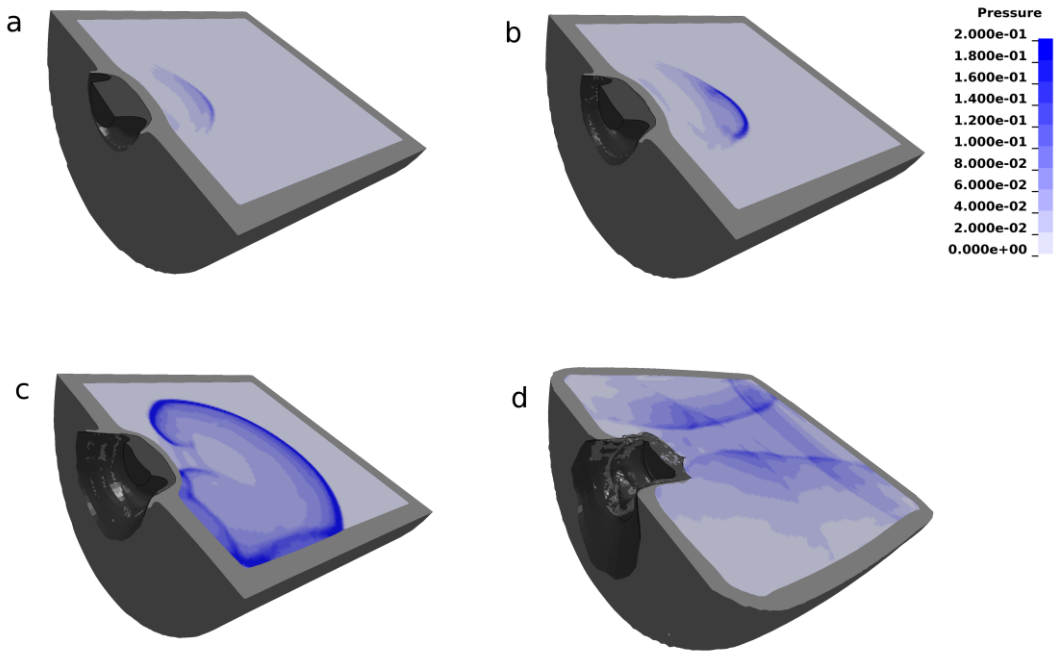

Figure 4. Simulation of a tilted fragment impacting a cylindrical charge. Snapshots of the burn wave is illustrated at different times 6 μs (a), 8 μs (b), 12 μs (c) and 20 μs (d) after impact.

Figure 4 shows snapshots from the simulation. At 6 μs (a) after impact, the shock wave has travelled about 2 cm into the explosive and the pressure starts to build up due to exothermic reaction. 2 μs later (b) the reaction has accelerated and all the explosive is decomposed in the burn wave. The emerging detonation wave is clearly skew due to the fragment yaw. This asymmetry around the z-axis (along path of fragment) has the consequence that the casing starts to expand about 2 μs later on one side of the charge as confirmed by the snapshot at 12 μs (c). Finally, Figure 4d shows the charge 20 μs after impact when expansion of the casing has begun. The result shows that this ignition and growth parameter set predicts a delayed detonation and we can expect the simulated critical velocity to be somewhere below 1700 m/s.

This type of model can in principle be used to investigate detonation build-up, study the effect of fragment yaw and non-centred impact or predicting a critical fragment velocity for a particular charge. Here, the model is used to test the accuracy of an Ignition and growth parameter set calibrated against both instrumented gap tests and rate stick tests.

Table 1. Fragment velocity and tilt in vertical plane estimated from high-speed recordings.

Test number	velocity	Tilt
	m/s	Degrees
4	1306	0.58
7	1819	1.68
8	2125	0.95

RESULTS AND DISCUSSION

First, we present the high-speed video recording of each test. The fragment velocities are calculated from the 10 frames that show the fragment prior to impact. In Table 1 we presents the fragment velocities and estimated yaw angles. For an RDX-based explosive like PBXN-109, we expect no or very mild reaction at fragment velocity 1306 m/s and full detonation at 2125 m/s.

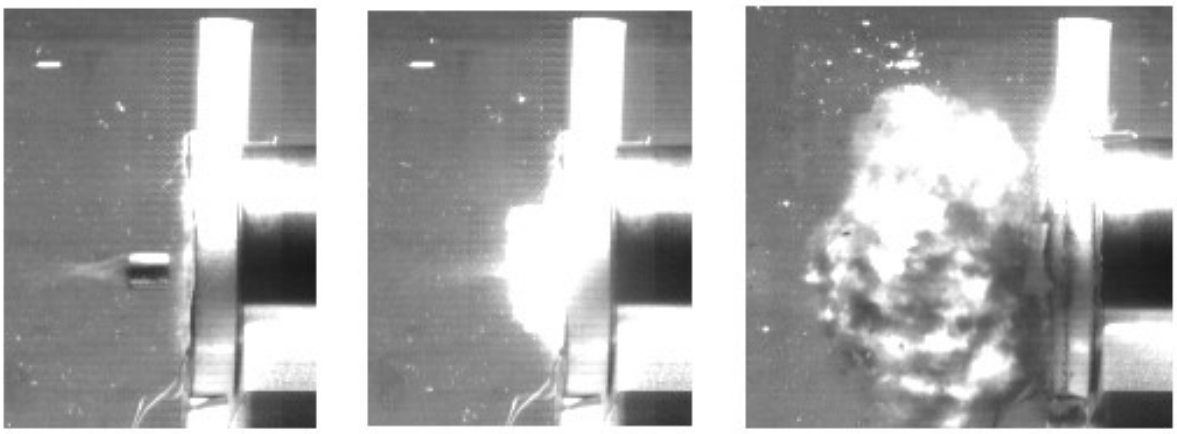

Figure 5. Snapshots from high-speed filming just before impact (left) at impact (middle) and approximately 100 µs after impact (right) for fragment velocity 1306 m/s.

Figure 5 shows three snapshots from the 1306 m/s test: just before impact (left), just after impact (middle) and approximately 100 µs after impact (right). Upon impact, light is generated as the fragment penetrates the steel casing. Subsequently, mostly unreacted explosive is ejected in a plume directed opposite to the path of the fragment. The degree of reaction is very limited, which is confirmed by inspection of the charge after the test.

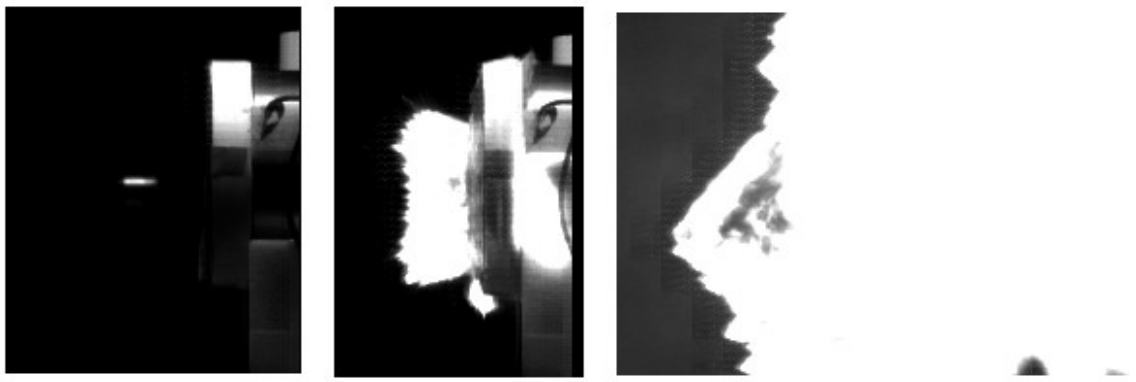

Figure 6. Snapshots from high-speed filming just before impact (left) at impact (middle) and approximately 100 µs after impact (right) for fragment velocity 2125 m/s.

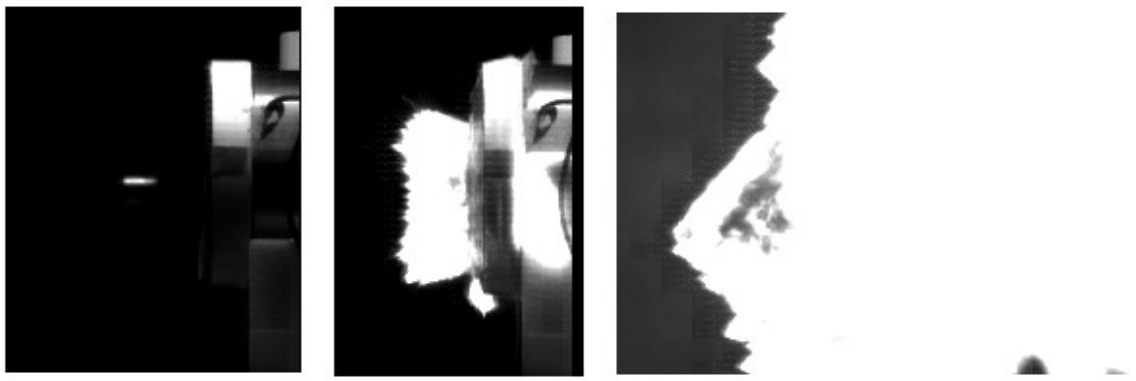

Figure 7. Snapshots from high-speed filming just before impact (left) at impact (middle) and approximately 100 µs after impact (right) for fragment velocity 1819 m/s.

Figure 6 and Figure 7 indicate that detonation occurs in the 2125 m/s and 1819 m/s tests. This is supported by blast pressure measurements and charge fragment analysis.
The snapshots before impact in Figure 5, Figure 6 and Figure 7 provide information on position and orientation of the fragment in the vertical plane. In the 1306 m/s and 2125 m/s, the point

of impact is close to the centre of the charge (in the vertical direction). In the 1819 m/s test, the point of impact is below the center (approximately 15 mm).
In all three tests, the fragment seems to be well-aligned in the vertical plane, e.g. very little projectile yaw has occurred over the 8 m flight. Table 1 summarizes projectile yaw estimated from video snapshots. The 3D model can be used to estimate the effect of fragment yaw on the critical velocity. Simulations with tilts of 2-3˚ in one direction and 2 directions has a negligible effect on the resulting critical velocity. A significant effect appears at 5-10 degrees tilt. At a fragment tilt of 10˚, the simulated critical velocity is increased from 1670 m/s to above 1800 m/s.
The PDV signal which corresponds to the initial velocity of the charge casing at a certain point is however considered the primary data for validation since a direct comparison to simulation is possible.

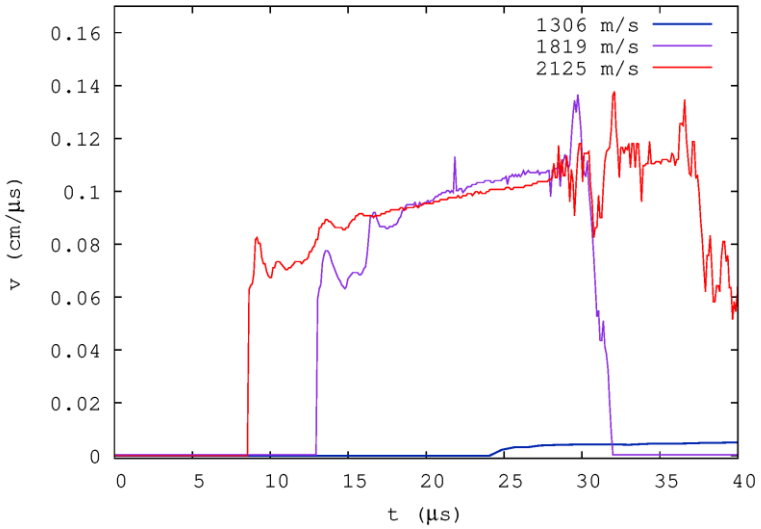

Figure 8. Measured wall expansion velocity for the three tests with fragment velocities 1306 m/s (blue), 1819 m/s (purple) and 2125 m/s (red).

Figure 8 shows the PDV signals for the three fragment impact tests. The qualitative interpretation is clear; at fragment velocity 1306 m/s the expansion velocity is low (about 35 m/s) whereas for the two higher fragment velocities the expansion velocity is about 20 times higher. The signals from the two higher fragment velocities bear a clear resemblance to the expansion velocity in a typical cylinder test. The sudden jump-off up to about 0.07 cm/µs thus provides a signature of detonation. The 1819 m/s and the 2125 m/s signals have similar profiles except for a temporal shift of 4.5 µs. A plausible explanation for this is that the build-up to detonation is slower in the 1819 m/s test. A more detailed analysis of this is presented below together with the model validation.

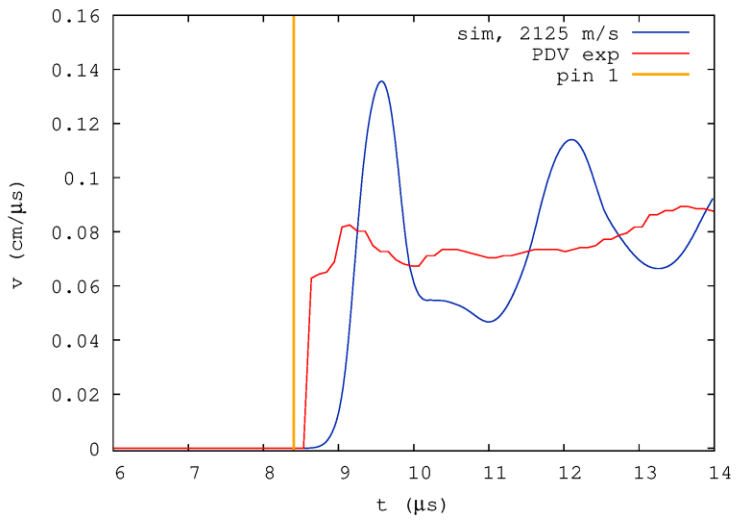

Figure 9. Measured expansion velocity (red), measured time of arrival (orange) and simulated expansion velocity (blue) at fragment velocity 2125 m/s.

Figure 9 shows casing response at a fragment velocity of 2125 m/s. First, we can note that the arrival time of the shock wave in the casing at the position of the PDV-probe (red curve) is close to the arrival time at the pin on the opposite side (orange vertical line). This, together with the snapshots from the high-speed video recording, indicates that the point of impact is well-centred on the charge.

In the simulation of the 2125 m/s test, close to prompt detonation results in a shock wave that arrives at the PDV location on the casing at just before 9 µs. The experimental jump-off occurs 400-500 ns earlier. This shows that the run distance to detonation is short and that this velocity is well above the critical velocity for detonation.

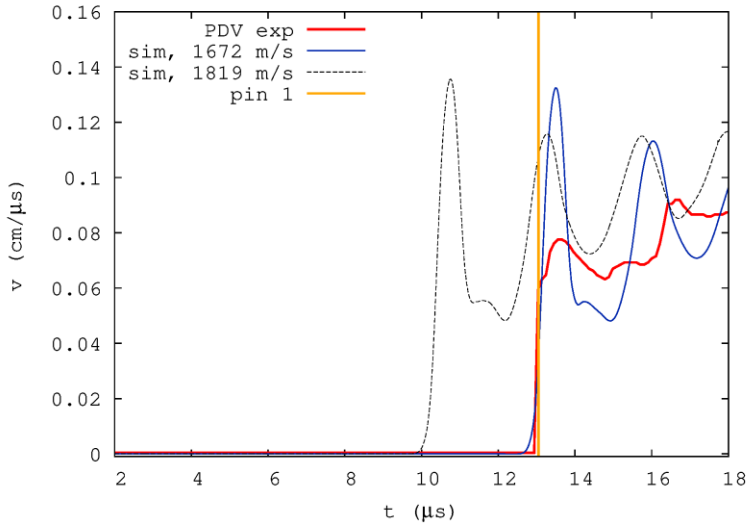

Figure 10. Measured expansion velocity (red), measured time of arrival (orange) at fragment velocity 1819 m/s and simulated expansion velocity at fragment velocity 1819 m/s (black, dotted) and 1672 m/s (blue).

Figure 10 shows casing response at a fragment velocity of 1819 m/s. The time of arrival at the pin (opposite the PDV) indicates symmetry in the horizontal plane. However, the high-speed recording showed that the impact point is below the centre point on the charge (in the vertical direction). A geometrical estimate shows that an impact point 15 mm below the centre point on the charge yields an additional distance of 2.3 mm (compared to a perfect centre-hit) in the explosive, corresponding to a delay of 300 ns assuming a detonation

velocity of 7.65 cm/μs. The simulated PDV signal at 1819 m/s (black, dotted) predicts expansion to start at about 10 μs after impact. This is 3 μs earlier than experiment (red), indicating that the calibrated parameter set predicts a higher sensitivity to shock than what we see in this fragment impact test. If we reduce the impact velocity in the simulation, the jump-off of the casing will be delayed until the critical velocity is reached and expansion velocity fall of drastically. We find that an impact velocity of 1672 m/s results in the best fit to the experimental curve. This is just above the critical velocity in the simulation. This analysis implies that the calibrated parameter set under-predicts the critical velocity for detonation with 147 m/s.

CONCLUSIONS

Three tests were performed with fragment velocities 1300 m/s (well below predicted threshold), 1820 m/s (around simulated threshold) and 2125 m/s (well above predicted threshold). An evaluation of the tests are presented with respect to high-speed video recordings and PDV signal. This evaluation clearly indicates that the second test, with fragment velocity 1820 m/s, is just above the threshold for detonation.
The PDV probe, directed towards the casing sidewall, provides a clear signature the arrival of the shockwave/detonation front. In particular, the two tests with the highest fragment velocities show expansion velocities indicating detonation. However, for the highest velocity (2125 m/s) comparison to the hydrocode simulation shows that prompt detonation occurs whereas the detonation is delayed for the 1820 m/s test.
The validation of the previously calibrated reactive burn model shows that the model under-predicts the critical velocity for detonation with about 150 m/s. We conclude, in line with a parallel study [4], that it may be challenging to capture fully the radial effects present in a fragment impact test by calibrating against planar gap tests and that rate stick data from steady state is insufficient for this purpose. Nevertheless, initiation tests with a non-planar set-up (similar to the fragment impact test) can be used to improve the predictive power of a reactive burn model.

[1] E. L. Baker, N. Al-Shehab, K. Miers, and D. Pudlak, "Insensitive Munitions Fragment Impact Gun Testing Technology Challenges," *Propellants, Explosives, Pyrotechnics,* vol. 41, pp. 572-579, 2016.

[2] M. Bergh, R. Wedberg, and J. Lundgren, "Optimization of Equation of State and Burn Model Parameters for Explosives," *APS Proceedings,* 2018.

[3] G. S. Wang, "Characterization of Strength and Fracture Properties of S355-J2 Steel," FOI-R--4470--SE, 2017.

[4] M. Bergh, A. Helte, O. Andersson, and A. Odell, "Effect of Pressure Pulse Duration and Lateral Distribution on Fragment Impact Initiation of High Explosives," in *International Detonation Symposium*, Chesepake Bay, 2018.